Relationship between sawtooth events and magnetic storms

X. Cai,[1] J.-C. Zhang,[2] C. R. Clauer,[1] and M. W. Liemohn[3]

Received 22 November 2010; revised 5 April 2011; accepted 14 April 2011; published 12 July 2011.

[1] The relationship between sawtooth events and magnetospheric substorms has been discussed extensively. However, the relationship between sawtooth events and magnetic storms has not been systematically examined. Using the sawtooth event list and magnetic storm list from January 1998 to December 2007, we investigate whether sawtooth events are storm time phenomena and whether there is a dependence on the strength and phase of storms. We have found that most of sawtooth events occur during storm time. Nevertheless, there are still 6 sawtooth events (5.4% of total events) that occur during nonstorm intervals. Sawtooth events also tend to occur during intense storms, with an occurrence rate of 63.5%. Sawtooth events can initiate during any stage of storms, however 55.9% of sawtooth events occur during the storm main phase through the time the ring current reaches its maximum strength. Therefore we conclude that sawtooth events are very often but not necessarily storm time phenomena. And not all storms contain sawtooth events. We suggest most sawtooth events occur during a special subset of storms that have just the right driving conditions to set intense, periodic, near-tail magnetic reconnection bursts.

Citation: Cai, X., J.-C. Zhang, C. R. Clauer, and M. W. Liemohn (2011), Relationship between sawtooth events and magnetic storms, *J. Geophys. Res.*, *116*, A07208, doi:10.1029/2010JA016310.

1. Introduction

[2] Sawtooth events were first described as a series of particle injection events by *Belian et al.* [1995]. Compared with typical magnetospheric substorms, the sawtooth particle injection is observed to occur over a wider local time extent nearly simultaneously.

[3] Sawtooth events are characterized by two features shown in particle injections: wide local time extent and quasiperiodic oscillations. *Henderson et al.* [2006a] pointed out that the injections appear "simultaneously" only because they are typically plotted in a large time window, e.g., 24 h. When plotted in a small time window, e.g., approximately hours, the injections show time delays between satellites and also energy dispersed patterns for satellites outside the injection boundary, which are typical features during magnetospheric substorms. The sawtooth injection boundary, however, is unusually large and can include the entire nightside extending past the terminators. Since particle injection is a typical feature during magnetospheric substorms [e.g., *Arnoldy and Chan*, 1969], there are efforts trying to determine whether sawtooth events are just a series of substorms or they are new phenomena, as a new mode of magnetospheric convection. *Henderson* [2004] proposed that they are similar to substorms, except the particle injection boundary and the near-Earth reconnection site are closer to the Earth than that during typical substorms. While this can explain the wide injection boundary, why they occur periodically still requires more investigation. *Cai and Clauer* [2009] reported that the average sawtooth period is 179.6 min, with a large standard deviation, which is 54.0 min. Sawtooth events are rather quasiperiodic instead of periodic phenomena. Currently there are two different explanations: (1) sawtooth events can be triggered by solar wind discontinuities, for example, pressure jumps [*Lee et al.*, 2004] and/or interplanetary magnetic field (IMF) changes [*Henderson et al.*, 2006a] and (2) the period of sawtooth events is related to an intrinsic period of the Earth's magnetosphere and is independent of external solar wind drivers [*Huang et al.*, 2003a; *Henderson et al.*, 2006a]. On the other hand, *Borovsky et al.* [2009] claimed that sawtooth events are a special phenomena and are associated with unique solar wind conditions, during which the Alfvénic Mach number M_A is low. They also believed that sawtooth particle injection is globally dispersionless, even around the local noon.

[4] The solar wind drivers during sawtooth events have been examined statistically by *DeJong et al.* [2008] and *Partamies et al.* [2009]. From the histograms of solar wind density, temperature and magnetic field strength, they found that solar wind driving conditions during sawtooth events are stronger than those during typical substorms and steady magnetospheric convection events (or balanced reconnection intervals, [*DeJong et al.*, 2008]). The statistical characteristics of the solar wind agree with those during an

[1]Bradley Department of Electrical and Computer Engineering, Virginia Tech, Blacksburg, Virginia, USA.
[2]Space Science Center, University of New Hampshire, Durham, New Hampshire, USA.
[3]Department of Atmospheric, Oceanic and Space Sciences, University of Michigan, Ann Arbor, Michigan, USA.

0148-0227/11/2010JA016310

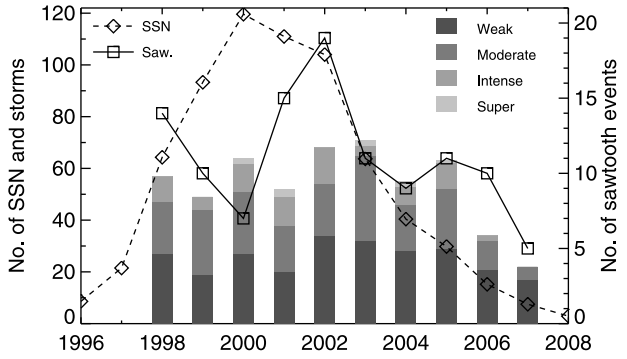

Figure 1. The numbers of sawtooth events and magnetic storms of different strength and yearly sunspot numbers (SSNs) from 1998 to 2007. The SSNs for solar cycle 23 are shown from 1996 to 2008. The SSNs are plotted as diamonds and connected with the dashed line. The number of sawtooth events is shown as rectangles and connected with solid line. During each year, the number of storms of different strength are illustrated as vertical bars in different shades. The SSN and number of storms share the left *Y* axis. The right *Y* axis is for the number of sawtooth events.

interplanetary coronal mass ejection (ICME). Since it is well known that ICMEs are capable of driving magnetic storms [e.g., *Gonzalez et al.*, 1999], there is a hypothesis that sawtooth events are storm time phenomena.

[5] However there has been little effort to test this hypothesis due to the lack of a comprehensive sawtooth events list and magnetic storms list. Using the sawtooth event from *Cai and Clauer* [2009] and our magnetic storms list, which covers from January 1998 to December 2007, we will test the hypothesis from the following aspects: (1) are sawtooth events storm time phenomena, (2) is there a sawtooth interval during each storm regardless of storm strength, (3) does the sawtooth occurrence rate depend on the strength of the ring current, and (4) is there a preferred storm phase for sawtooth occurrence?

2. Methodology

[6] The sawtooth event list to be used here is from *Cai and Clauer* [2009], who include 111 sawtooth intervals and 438 individual teeth from January 1998 to December 2007. The criteria for events to be included in this list are (1) the injections are observed quasiperiodically and (2) the particle injections are observed both around the local noon and local midnight (±3 magnetic local time hours).

[7] Magnetic storms are identified using the hourly disturbed storm time (*Dst*) index from the World Data Center for Geomagnetism in Kyoto, Japan. From January 1998 to December 2003, the *Dst* index values are the final *Dst* index. While from January 2004 to December 2007, the *Dst* index values are the provisional version. The contribution due to solar wind dynamic pressure P has been removed using the formula $Dst^* = Dst - 7.26\sqrt{P} + 11$ [*O'Brien and McPherron*, 2000], where P is in nPa. If solar wind density or velocity measurements are missing, *Dst* is substituted for *Dst** (hereafter *Dst*). The magnetic storms between January 1998 and December 2007 are classified into four categories based on the work by *Gonzalez et al.* [1994]. During storm intervals, the *Dst* index must be equal to or less than −30 nT. During weak storms, the minimum *Dst* is between −30 and −50 nT. During moderate storms, the minimum *Dst* is between −50 and −100 nT. As for intense storms, the *Dst* is between −100 and −250 nT. Super storms are those intervals when the *Dst* is less than −250 nT. During the period we are interested in, we have found 535 storms in total. There are 254 weak storms, 197 moderate storms, 74 intense storms and 10 super storms.

[8] As the averaged sawtooth period is about 3 h [*Cai and Clauer*, 2009], over the *Dst* index we also plot the symmetric disturbance field in the horizontal (dipole pole) direction, the *SYM-H* index. The statistical study by *Wanliss and Showalter* [2006] found that a very high correlation coefficient between the *SYM-H* and *Dst* indices, which is above 0.9, though the deviations between *Dst* and *SYM-H* vary with the strength of storms. Even during intense storms, the deviations are usually less than 20 nT. They had concluded that *SYM-H* index can be used as a high-resolution version of the *Dst* index. We use the provisional *SYM-H* index also downloaded from the World Data Center for Geomagnetism in Kyoto, Japan.

[9] To help understand the *Dst* and *SYM-H* index variations, we have examined the 1 min resolution propagated solar wind data measurements from the ACE satellite. The data are obtained from the OMNI data set, which is provided by the Goddard Space Flight Center, and have been propagated to the bow shock nose 17 R_E with the minimum variance method [*Weimer and King*, 2008].

3. Sawtooth Occurrence and Storm Strength

[10] The time interval we have examined here covers almost the whole solar cycle 23, which started in May 1996 and ended around December 2008. The interval includes the solar ascending phase, solar maximum and solar descending phase. Figure 1 shows the number of sawtooth events and storms with different strength from 1998 to 2007. The yearly sunspot numbers (SSNs) are also plotted. The number of storms has no clear dependence on the SSNs, though there are less storms around solar minimum 2007. There are slightly more storms and especially intense storms around the solar maximum and initial descending phase, which means that the solar wind structures around those periods are more geoeffective than those during other periods of solar cycle 23. This two-peak feature has been seen by *Gonzalez et al.* [1990] during solar cycle 20 and 21. They suggest that the peaks correspond to the similar dual-peak distribution of B_s fields with intensities larger than 10 nT and durations longer than 3 h.

[11] There is no clear trend between solar activity and the number of sawtooth events, other than that the occurrence of sawtooth events has one maximum and two apparent minimums. The number of sawtooth events reaches its maximum in the initial descending phase in 2001 and 2002. One of the occurrence minimum is around the solar minimum in 2007. The other one is around the solar maximum in 2000, during which the solar wind is very active and is dominated by ICMEs [*Gonzalez et al.*, 1999]. One possible explanation is that the magnetosphere is a nonlinear system, or a chaotic system when the solar wind energy rate is larger than a threshold [*Baker et al.*, 1990]. It transitions from a

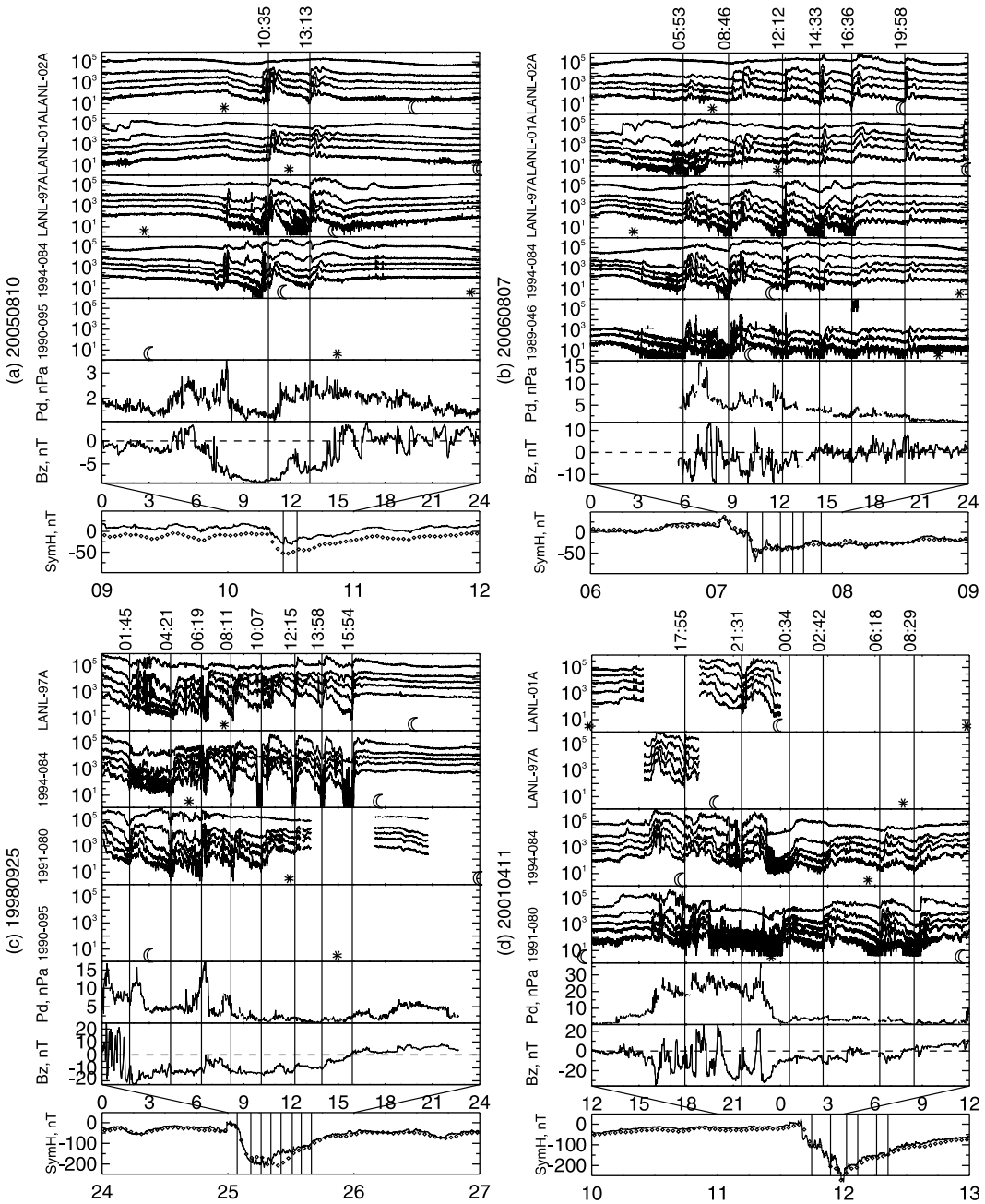

Figure 2. The sawtooth events occurred during (a) a weak storm, (b) a moderate storm, (c) an intense storm, and (d) a super storm. From the top to the bottom for each storm type, the daily energetic proton fluxes measured by Los Alamos National Laboratory (LANL) satellites and propagated solar wind dynamic pressure P_d and IMF B_z are plotted. Local noon and local midnight of LANL satellites are represented as stars and moons. To show the overall ring current variation pattern, the *SYM-H* index and hourly *Dst* index are plotted 1 day before and after the sawtooth day. The *SYM-H* index is plotted as a solid line and *Dst* is plotted as diamonds. The onset of each individual tooth is illustrated as a vertical line, with the universal time indicated.

predictable and periodic magnetosphere to an aperiodic and quasi-random magnetosphere [*Shaw*, 1984].

[12] After examining the ring current strength during each sawtooth interval, we find that sawtooth events can occur during storms with any strength. Figure 2 shows 4 sawtooth examples that occur during various levels of storm activity: a weak storm (event a), a moderate storm (event b), an intense storm (event c), and a super storm (event d). We only show the solar wind dynamic pressure P_d and IMF B_z. To show the overall ring current development and decay, the *SYM-H* and *Dst* are plotted 1 day before and after the sawtooth day.

[13] Now we will discuss Figure 2 in detail. Generally speaking, the *SYM-H* index and *Dst* index agree with each

other well. There are, in general, discrepancies in some of the small details as the *SYM-H* index has higher time resolution and is calculated from more ground magnetometers, compared to *Dst* index. The difference in Figure 2a, however, is large, measuring about 20 nT. Even considering solar wind pressure corrections to *Dst* index [*O'Brien and McPherron*, 2000], which only decreases the difference by 0.7 nT as P_d is around 2 nPa, the difference is still large. One possible reason is both the *Dst* index and *SYM-H* index are provisional indices and lack adequate corrections. The quiet day baseline used for the two calculations is clearly different. Figure 2a shows a sawtooth event during a weak storm. The first tooth seems initiated with a pressure drop around 0800 UT, as the magnetosphere changed its configuration due to the pressure change. However, the onset which was around the minimum of the *Dst* disturbance seems to be triggered by the pressure increase at 1035 UT. The second tooth was during the recovery phase. The IMF northward turning might trigger another local substorm as seen by Los Alamos National Laboratory (LANL) satellite LANL-97A. The sawtooth event b occurred during a fluctuating IMF B_z interval. It started in the main phase and extended to the recovery phase. The first onset seems corresponded to a pressure impulse. However, there are no clear relationships between subsequent onsets and solar wind changes. The third sawtooth (event c) occurred during an ICME. The sawtooth event interval included the peak of the ring current and extended well into the slow recovery phase. After the IMF B_z turned northward, the oscillation stopped. Figure 2d shows the first two teeth on 11 April 2001 and the subsequent teeth on 12 April 2001. The first tooth was triggered by the solar wind pressure impulse. However the subsequent onsets had no clear one-to-one relationship with IMF or pressure changes. The sawtooth interval included the storm main phase and recovery phase. During the second tooth, the dayside magnetosheath was pushed inside geosynchronous orbit as the pressure was large. The LANL satellite 1991-080 was situated in the magnetosheath region from 1930 UT to 2330 UT.

[14] Sawtooth events are also found during nonstorm time. Figure 3 shows all six sawtooth events during intervals without storms between January 1998 and December 2007. The propagated solar wind drivers for those six events are plotted in Figure 4. For these events, the ring current intensity does not increase and decay as that during a typical magnetic storm [*Gonzalez et al.*, 1994]. Although there are discrepancies between *Dst* and *SYM-H* index during sawtooth events d and e, these errors will not effect our investigation as we are only looking for the trend of the ring current. The six sawtooth events could be further grouped into two types based on ring current strength and solar wind drivers: (1) sawtooth events with weak ring current during weak or moderate solar wind driving (i.e., events a, c, e, f), and (2) sawtooth events with enhanced ring current during moderate or strong solar wind driving(i.e., events b, d). The threshold of ring current is set to around −50 nT. For the first type of events, the solar wind drivers may not be capable of driving magnetic storms. For example, IMF B_z is weak and turbulent (events a, e), or IMF B_z is moderate but short (events c, f). However, it is unclear why there is no magnetic storm for the second type of events, though the solar wind drivers are moderate (event b) or even strong (event d). Before the start of 10 September 2002 sawtooth event, IMF B_z stayed approximately steady at −5 nT for 9 h. The first onset was probably initiated by a pressure impulse and further IMF B_z enhancement. The ring current kept at a constant level before the sawtooth event and gradually increased during the sawtooth interval. Then it slowly recovered after IMF B_z northward turning. As the ring current changed by less than 25 nT during the whole interval, no magnetic storm could be identified.

[15] Figure 5 shows the statistical analysis of sawtooth occurrence rates during storms with different strength. From January 1998 to December 2007, we found 111 sawtooth events and 535 magnetic storms. As shown in the pie charts, most of the sawtooth events occurred during magnetic storms, especially during intense storms. The sawtooth event occurrence rate during intense storms is 63.5%, which means 63.5% of intense storms are accompanied with sawtooth events. The occurrence rates for weak storms and super storms are approximately the same. Sawtooth events are less likely to occur during weak storms. There are still 6 sawtooth events, which is 5.4% of total events, that occurred during nonstorm times. Therefore, sawtooth events are likely but not necessarily storm time phenomena. And clearly not all magnetic storms are accompanied by sawtooth intervals.

4. Sawtooth Occurrence and Storm Phase

[16] As mentioned before, a typical storm consists of initial, main and recovery phases. It is not clear whether sawtooth event occurrence has a phase preference. To examine this, we have classified sawtooth events that occurred during storms into three categories depending on whether the *Dst* minimum is before, during or after the sawtooth interval. If the minimum is after the end of the sawtooth interval, the sawtooth events is in the main phase. If it is during the interval, then the sawtooth event is around the minimum. If *Dst* minimum is before, then the event is in the recovery phase.

[17] Figure 6 gives examples of the three categories. A sawtooth event that occurred at the beginning of the main phase is shown in Figure 6a. Following the initial phase which is also called the storm sudden commencement (SSC) around 1500 UT on 17 August, the ring current started to develop as shown in *SYM-H* plot. There was another SSC around 0100 UT on 18 August due to the sudden solar wind pressure jump. After that, the magnetosphere entered sawtooth oscillation mode. The ring current kept approximately steady. Then the magnetosphere became active and chaotic which indicates the end of the sawtooth interval. The ring current reached its maximum around 1500 UT and gradually recovered afterwards. Figure 6b gives a sawtooth example during the peak of an intense storm. This storm had a weak initial phase as the pressure jump was only around 3 nPa. The continuous intensification of the ring current was associated with quasi-steady southward IMF B_z from 0130 UT to 0530 UT. The first sawtooth onset was triggered by the IMF northward turning around 0530 UT and the ring current decayed. Even though there were southward intervals after 0800 UT, which intensified the ring current slightly, these did not change the overall recovery trend. Figure 6c is a sawtooth

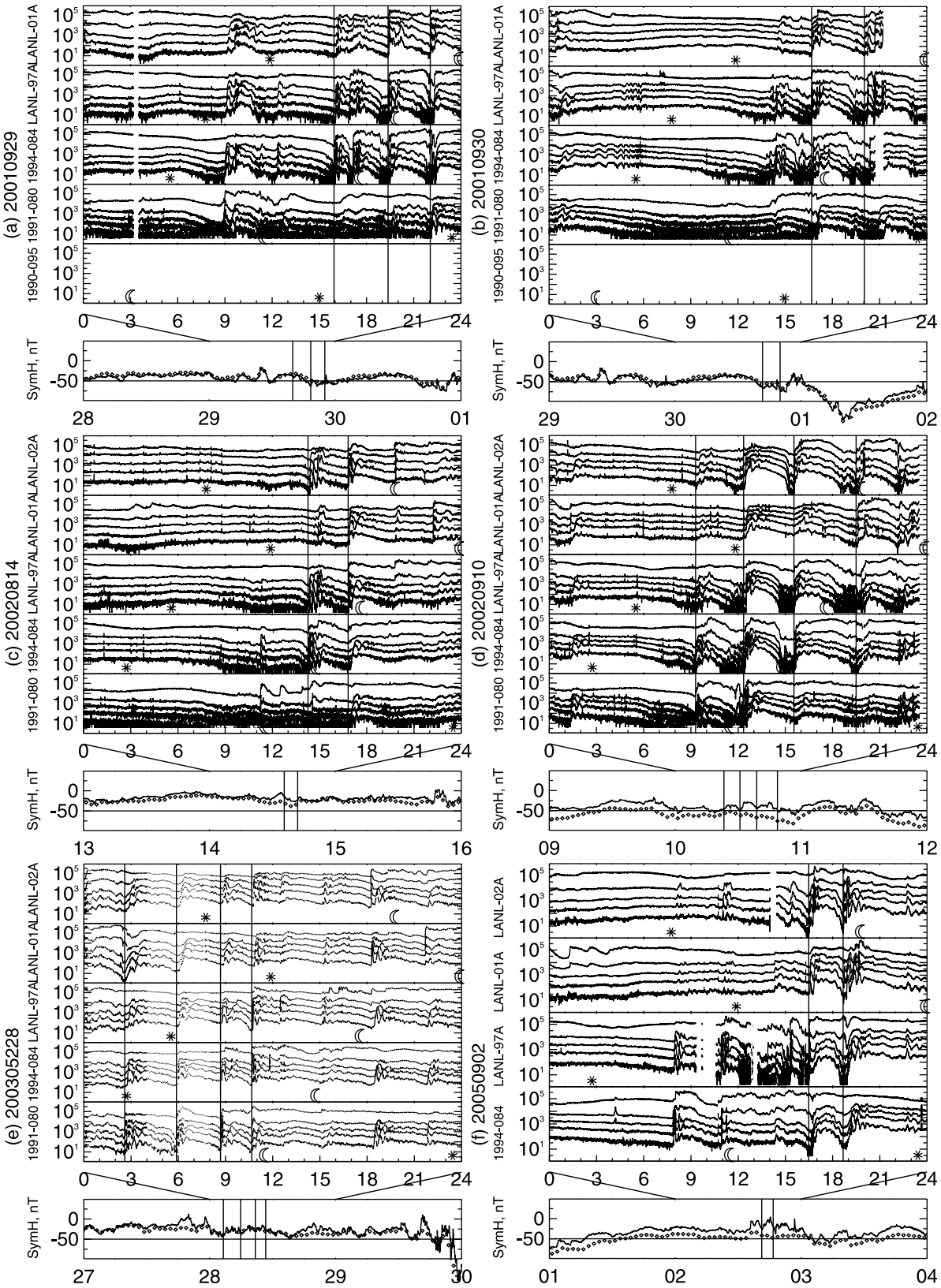

Figure 3. Six sawtooth events during nonstorm intervals. The format is the same as that in Figure 2 except that the propagated solar wind drivers are shown instead.

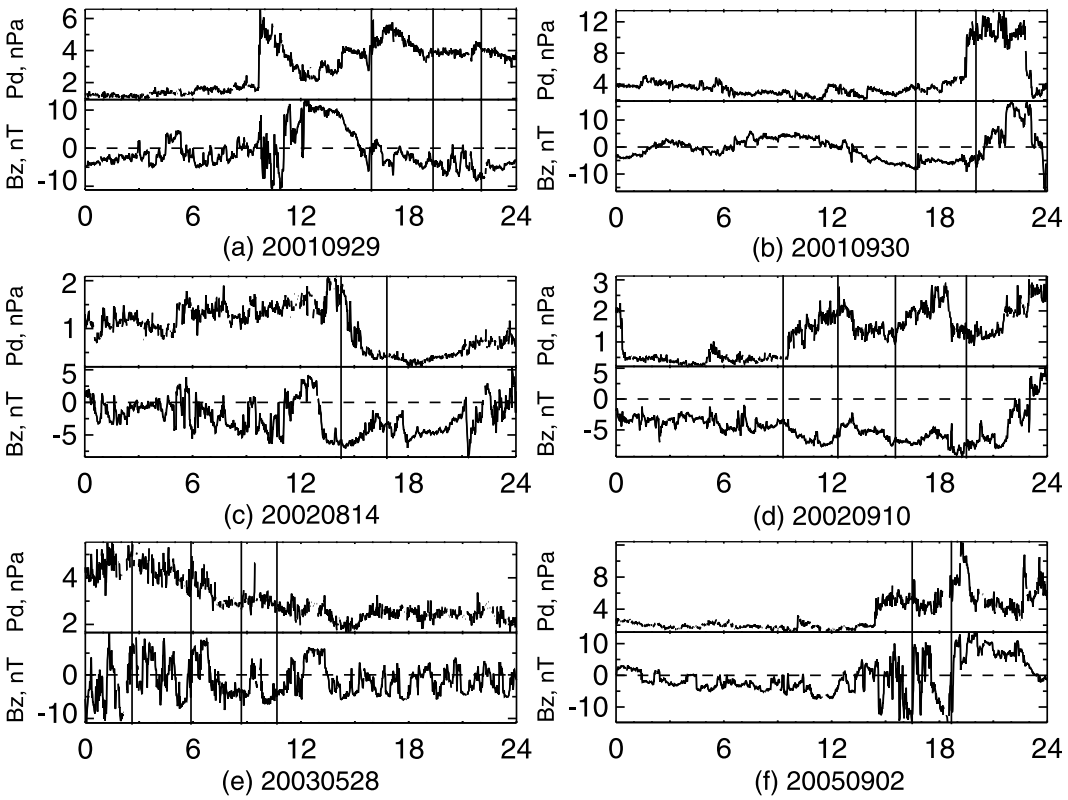

Figure 4. Propagated solar wind dynamic pressure P_d and IMF B_z for the six nonstorm sawtooth events shown in Figure 3. The vertical lines mark the onset of each individual tooth. Note that the ranges of P_d and B_z are different from plot to plot.

example during the recovery phase of an intense storm. After reached its maximum, the ring current decayed gradually while the IMF B_z was near 0 nT for several hours on 22 October 2001. The sawtooth interval began when the IMF B_z turned southward around 1100 UT. During the sawtooth interval, *Dst* was approximately constant. The ring current decay rate seems to be balanced by the growth rate, which was supposed to increase as a result of strong southward IMF B_z.

[18] The statistical results are shown in Figure 7. Sawtooth events can occur during any phase of a magnetic storm. However, more than half of sawtooth events, 55.9%, occur during the intervals when the ring current reaches its maximum strength. There are examples, however, in which sawtooth intervals straddling the peak are almost entirely during the main phase or recovery phase. One conclusion is that sawtooth events can occur during any part of a magnetic storm. The occurrence of sawtooth has no direct relationship with ring current strength.

5. Discussion

[19] From the examples above, we come to several important conclusions. Figure 2c shows a sawtooth event during an ICME, while IMF B_z stayed strong southward for more than 10 h. The sawtooth interval stopped when IMF B_z turned northward. If sawtooth events can be considered as a series of energy loading-unloading processes, the magnetotail has to gain energy before it starts to release energy, which means solar wind IMF should have southward

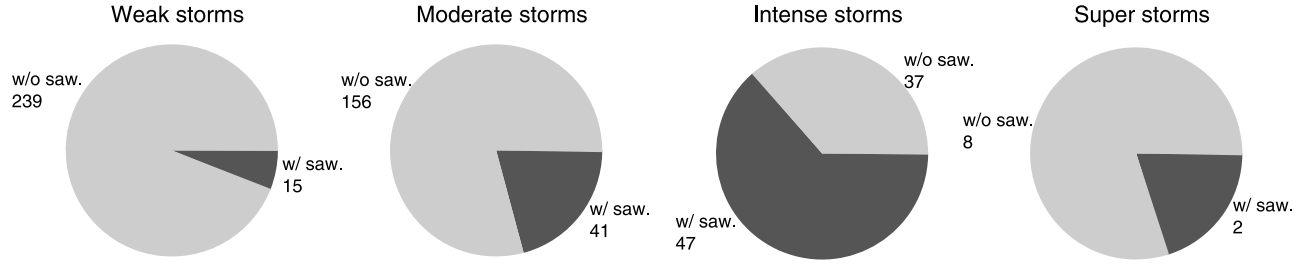

Figure 5. Pie charts of sawtooth occurrence rates during storms of different strength. The storms with sawtooth events and storms without sawtooth events are shaded in dark and light, respectively. Number of storms with sawtooth events and without sawtooth events is illustrated beside each pie chart.

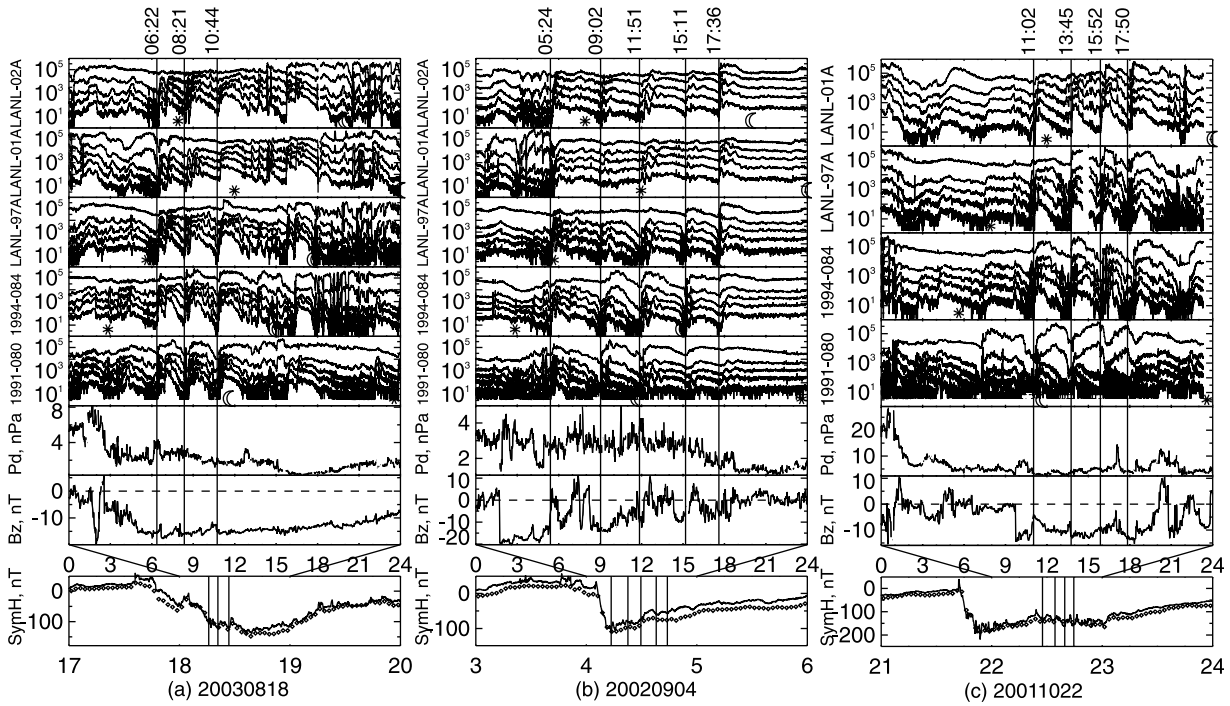

Figure 6. Examples of sawtooth events occurred at (a) the beginning of the main phase of a storm, (b) peak of a storm and (c) recovery phase of a storm. The format is the same as Figure 2.

intervals before any sawtooth event, no matter whether IMF B_z is continuous or fluctuating. Figure 3f presents a sawtooth event with weak ring current strength, which suggests that sawtooth occurrence does not require the development of the ring current. Figure 6c is a sawtooth event during the recovery phase of an intense storm, which seems counterintuitive. The occurrence was due to a long interval of strong southward solar wind IMF B_z. In this case, the deposited energy and dissipated energy was in balance in the near Earth region, as *Dst* stayed approximately constant during the sawtooth interval.

[20] Statistically, we find that about 96% of sawtooth events occur during magnetic storms of different intensity. However, there are still 6 events during nonstorm intervals. Sawtooth events can occur during storms with any strength, from weak storms to super storms. However, about 80% of sawtooth events occur during moderate storms and intense storms. The occurrence rate is the largest during intense storms, of which 63.5% contain sawtooth events. We conclude that sawtooth events are very likely but not necessarily storm time phenomena and not all magnetic storms contain sawtooth events.

[21] As pointed by *Kamide et al.* [1998], we need to keep in mind that geosynchronous orbit is a fixed radial distance rather than a fixed magnetospheric domain. And since there is no direct measurements of ion species from LANL geosynchronous orbit, it is unclear whether the enhancements measured at geosynchronous orbit is due to the solar wind origin ions, which are mainly protons, or the ionospheric origin ions, which are single charged oxygen ion (O^+). During quiet times, geosynchronous orbit is on the outside of ring current region. However, during active times, the particles from the tail can be convected inside geosynchronous orbit due to an enhanced electric field.

[22] To help understand the relationship, we suggest sawtooth events and storms may have fundamental differences in energy transport and particle acceleration. Magnetic storms are characterized by the decrease of the axial magnetic field component measured by ground magnetometers in the midlatitude and low latitude, followed by a subsequent recovery [e.g., *Chapman and Bartels*, 1940]. The decrease is due to the enhancement of the trapped magnetospheric energetic particle population in the radial distance of 2–7 R_E [*Gonzalez et al.*, 1994]. The particle energy range is about 10–300 keV. Later the axial component is found to be related to the total energy of the ring current particles [*Dessler and Parker*, 1959]. Therefore magnetic storms can be considered as intervals of enhanced population of ring current energy range particles at the trapped region.

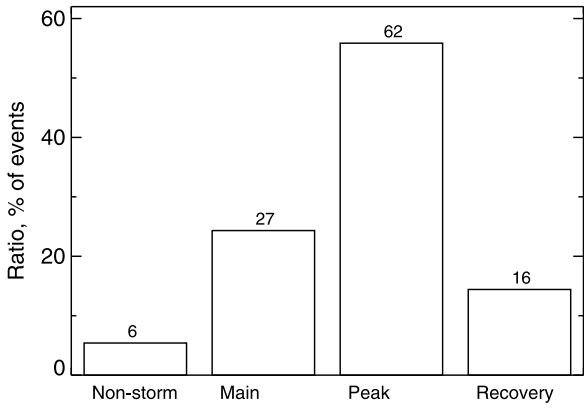

Figure 7. Number of sawtooth events occurred during each phase of magnetic storms and nonstorm time.

To understand storms, it is important to understand the processes that supply and remove the ring current particles between 2 and 7 R_E. Currently, there are two paradigms considering how the ring current builds up: (1) substorm particle injection and (2) enhanced convection due to a large solar wind electric field. While each paradigm is supported by data observations and simulations, it is also possible that both mechanisms contribute to the development of the ring current [*Reeves and Henderson*, 2001]. *Fok et al.* [1999] compared the total energy of proton during storms with and without substorm. They found that the particle injection into the inner magnetosphere has to be achieved by the coexistence of substorm processes and strong convection.

[23] Though there is no agreement on the fundamental physics of sawtooth events, it is starting to be accepted that sawtooth events are a series of energy loading-unloading processes, which result from a series of nightside magnetic reconnections. Originally sawtooth events are defined from their saw-blade variation trends, i.e., slow decreases followed by rapid recoveries, in the energetic proton (50–400 keV) differential energy fluxes observed at geosynchronous orbit. In our opinion, to understand sawtooth events, it is important to understand why the tail magnetic reconnections occur in a sequence, or why the magnetic lobes could accumulate magnetic fluxes several times after the previously stored magnetic energy is converted to kinetic energy through the reconnection process. From this aspect, we would suggest that sawtooth events are similar to a series of substorms, though the nightside reconnection site might be closer to the Earth and the subsequent substorms are embedded in the previous substorms. From the averaged global magnetic field tilt information at geostationary orbit from GOES, *Cai et al.* [2006a] found the first tooth during sawtooth interval behaves different from the subsequent teeth. The dayside magnetosphere, especially around local noon, during the first tooth is similar to that during isolated substorms. *Nagai et al.* [2005] pointed that the closer reconnection site events might be due to the strong solar wind driver. From the reconnection sites of 34 clear reconnection events determined from GEOTAIL data, they showed the radial distance of the sites is controlled by the efficiency of the solar wind energy input. The near-tail events, which are defined as the events with reconnection site between −15 R_E and −25 R_E, occur with large energy input. And the midtail events, with the site between −25 R_E and −31 R_E, occur with less energy input. The sites seem to show little dependence on solar wind pressure.

[24] If we consider sawtooth events as a series of energy loading-unloading processes, which are similar to substorms, it is possible that the frequent occurrence of particle injections during each tooth causes the intensity of ring current energy to build up and forms a storm main phase [*Akasofu*, 1964]. The fact that 96% of sawtooth events are occurred during magnetic storms supports this idea. However, as sawtooth events tend to occur during intense storms, it is also possible that both phenomena are driven by strong solar wind drivers.

[25] The fact that most sawtooth events occurred during storms hints that the solar wind driver that produces sawtooth events also tends to drive storms. That is to say, the solar wind drivers for the two categories should have an overlap. Most sawtooth events are probably special subset storms that have just the right internal conditions and the external driving conditions, for example, the high efficiency of solar wind energy input as pointed by *Nagai et al.* [2005], to set intense, periodic, near-tail magnetic reconnection bursts. It is true that both sawtooth events and intense storms could be driven by ICME and stream interactions [*Gonzalez et al.*, 1999; *Cai*, 2007]. It is well known that during the main body of an ICME, the IMF B_z may be steady and strong and solar wind speed is slow. During stream interactions, IMF B_z is typically fluctuating and solar wind speed is fast. Why both the steady and fluctuating IMF B_z can drive sawtooth events and storms is a mystery. One explanation is that the magnetosphere acts as a low-pass filter [*Clauer et al.*, 1981; *Ilie et al.*, 2010]. It is the total energy input integrated over a certain timescale that plays an important role.

[26] As discussed before, sawtooth events tend to occur during intense storms. During intense storms, enhanced O^+ is observed and the abundance increases with the intensity of magnetic storms. *Daglis and Kamide* [2003] proposed that existence of O^+ and subsequent inward substorm injection during storms would set a condition to cause a next substorm at a position closer to the Earth. In this paradigm, O^+ ions act as a catalyst for the inward invasion of substorm injection and play an important role in generating intense storms. Whether the occurrence of sawtooth events has a dependence on the O^+ abundance is unknown. Investigating the abundance of each ion species, especially O^+, during sawtooth events may help us answer this question.

[27] Although most sawtooth events occurred during storm time, there are nonstorm time sawtooth events. The strength of the ring current could be either weak or moderate during these events. When solar wind driving is weak, e.g., IMF B_z is less than −5 nT and also fluctuating, the magnetosphere may still enter sawtooth oscillation as it can load solar wind energy during those southward intervals. However, the weak electric field could not efficiently accelerate particles and transport them to the ring current region. Therefore there is no magnetic storm associated with the sawtooth event. We also note this type of sawtooth event could be directly driven, for example, the two onsets of sawtooth event shown in Figure 3e clearly corresponded to the IMF B_z northward turnings. On the other hand, when solar wind driving is moderate or strong, especially it stays about constantly south for hours, the magnetosphere could be in an enhanced convection state without storms. The following solar wind changes or discontinuities, e.g., IMF B_z northward turnings, could initiate a sawtooth event interval. The magnetotail is experiencing a series of energy loading and unloading until no further energy loaded from solar wind. Furthermore, for the 18 April 2002 sawtooth event, *Liemohn et al.* [2007] found discrepancies between data-model comparisons of the ring current as seen by ENA imaging and that inferred from the *Dst* index. Their results imply that the ring current may not be greatly influenced by the sawtooth injections.

[28] Clearly there are storms without sawtooth events. However, the reason behind this is unclear. Here we provide two possible explanations. First, there might be a solar wind driver threshold for sawtooth events. If the solar wind driver is too weak, the accumulated magnetic flux in the lobe regions could be lost by local and small temporal scale

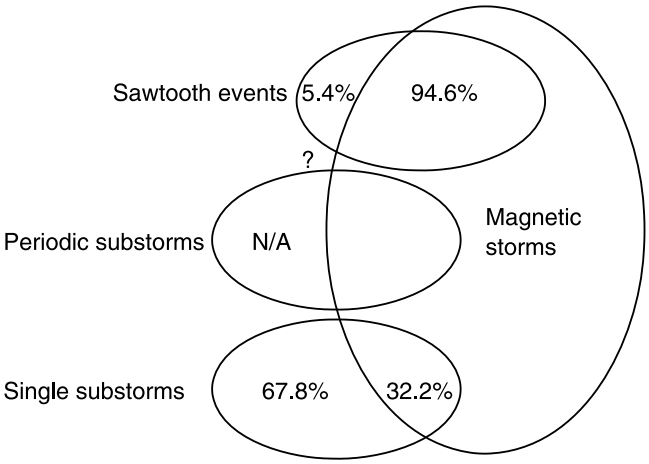

Figure 8. A diagram showing the relationships between magnetic storms and substorm family, which includes single substorms, periodic substorms, and sawtooth events. The percentage shows the ratio of individual events during nonstorm time and storm time. Plotting is not to scale.

events, i.e., busty bulk flows (BBFs), without a large scale reconnection event like substorms. If the solar wind driver is too strong, the whole magnetosphere becomes a chaotic system [*Baker et al.*, 1990]. In this case, the whole magnetosphere is in an active state and the stored energy dissipates in the manner of BBFs. It is thus impossible (or very unlikely) for the magnetosphere to release energy in large organized events like sawtooth events. Second, other than the magnitude of solar wind driver, the duration of southward IMF B_z might play an important role. For sawtooth events, continuous (not necessarily constant) energy needs to be deposited in the tail. However, for a magnetic storm, even an hour of strong southward IMF which results in a strong duskward electric field can accelerate particles in the distant tail and transport them to the inner magnetosphere. After the driver turns down, the ring current decays and the magnetosphere recovers.

[29] We would suggest examining the interplanetary solar wind driver and even original solar sources, combining global magnetosphere data (e.g., near Earth orbital satellite data, ground magnetometer data, and radar data) to fully understand the driver mechanism of sawtooth events. Some specific questions are (1) does each southward IMF B_z interval cause sawtooth events or storms and is there any threshold on the duration and the magnitude, (2) if the solar wind driver is similar, whether the storms with sawtooth events are more severe than storms without sawtooth events, and (3) what are the common features for the solar wind driver during sawtooth events? The statistical study by *DeJong et al.* [2008] showed that during sawtooth events, the solar wind tends to have low proton temperature, high solar wind speed, strong IMF B_z and low Alfvénic Mach number. The questions proposed here will supplement their research as this work will start from solar wind driver and then examine the corresponding magnetospheric response. While the superposed epoch analysis they utilized provides common features of the solar wind driver, it might be misleading as they combined all the solar wind measurements regardless of specific solar wind structure during each individual event.

[30] As sawtooth events and storms are not necessarily related, the relationship between them is similar to that between substorms and storms. The storm-substorm relationship is a long-lasting controversial topic. *Kamide et al.* [1998] claimed that the occurrence of substorms is important in forming the storm time ring current, as the increased ionospheric ions observed during the main phase of storms are accelerated by substorm-associated electric fields. Therefore it is believed that all storms should be accompanied with substorms. However, *Tsurutani and Gonzalez* [2006] showed a magnetic storm without substorms, which they defined as "convection events". Five out of 11 storms they had examined belong to this category. On the other side, there are quiet time substorms and storm time substorms [*McPherron and Hsu*, 2002]. Using ground magnetometer data, they have identified 166 nonstorm time substorms, which is 67.8% of total events, and 79 storm time substorms. Considering these facts, *Tsurutani and Gonzalez* [2006] suggested that storms and substorms are separate magnetospheric dynamic processes.

[31] As pointed out in previous literature [e.g., *Henderson*, 2004; *Henderson et al.*, 2006b; *Huang et al.*, 2003b; *Pulkkinen et al.*, 2007; *Clauer et al.*, 2006; *Cai et al.*, 2006b; *Kitamura et al.*, 2005], sawtooth events share a lot of similarities with isolated substorms. This leads some researchers to believe that sawtooth events are not totally unknown or new phenomena. We suggest sawtooth events are part of substorm family, which also includes single substorms and periodic substorms. Single substorms consist of nonstorm substorms (or isolated substorm) and storm time substorms. The characteristic of single substorms is only one nightside reconnection. If there are a series of reconnections and the reconnection sites have the similar distances with single substorms, the interval is considered as a periodic substorm. If the reconnection sites are closer than those during single substorms, this leads to a sawtooth event. The definitions of periodic substorms and sawtooth events can be subjective. A practical distinction is to examine whether the local time extent of particle injection is larger than a certain value, e.g., 12 h. During periodic substorms, the particle injection is still confined around local midnight. However, during sawtooth events, the particle injection is seen even in the dayside hemisphere. They can be considered as a series of substorms, where the subsequent ones are embedded in the previous one. The relationship between periodic substorms and sawtooth events still needs further examination.

[32] Here we use a diagram in Figure 8 to show the relationship between substorm family and storms. There is an overlap between each substorm family member and storms. The percentages come from *McPherron and Hsu* [2002] and this work. There are arguments whether periodic substorms should be considered as sawtooth events or not. We have put a question mark in the plot. However, we would suggest separating them from sawtooth events.

[33] Now we would like to clarify a last question: are storms with sawtooth events and multiple-dip storms the same? *Huang et al.* [2004] examined the ring current strength during several sawtooth events. They found that the *Dst* increased significantly by 20–40 nT after each onset. Therefore the *Dst* profiles also show a saw-blade shape.

When identifying multiple dip storms, *Zhang et al.* [2008] considered only the intervals when *Dst* is stronger than −100 nT and also utilized the 3 h box-smoothed *Dst*. They also required certain dip depth and time separation. As the timescale of sawtooth events is 2–4 h [*Cai and Clauer*, 2009], the small timescale *Dst* variations are weakened and smoothed by the averaging process. So it is unlikely these variations will be considered as major dips of a storm. However a careful comparison of the lists of multidip storms and sawtooth events is needed to answer this question.

6. Summary

[34] Using the sawtooth event list and magnetic storm lists from January 1997 to December 2007, which covers most of solar cycle 23, we have examined the relationship between sawtooth events and magnetic storms.

[35] First, we found the numbers of sawtooth events and storms drop around solar minimum in 2007. The occurrence of sawtooth events, however, show a local minimum at solar maximum and peaks during the descending phase after the solar maximum around 2002. This hints that the geoeffective solar wind structures during the descending phase, which are mostly stream interactions, are effective at producing both sawtooth events and storms. While ICMEs around solar maximum are also able to produce a large number of storms and even super storms, they are less effective to produce sawtooth events. We propose that sawtooth events tend not to occur during very intense solar wind drivers, as the magnetosphere becomes a chaotic system and it is unlikely that it can load and unload energy in regular oscillation cycles.

[36] Second, while 94.6% of sawtooth events occurred during magnetic storms, there are still 6 events during nonstorm time. Sawtooth events are also able to occur during storms with different strength, from weak storms to super storms. However, 79.3% of sawtooth events are during moderate storms and intense storms. The sawtooth occurrence rate during intense storms is the largest, which is 63.5%. Evidently sawtooth events are not necessarily storm time phenomena and not all storms contain sawtooth events.

[37] Third, sawtooth events can occur during any stage of storms regardless of the strength of the ring current, though 55.9% of sawtooth events are found to include the time when the ring current reaches its peak. Therefore there is no requirement in ring current strength for sawtooth event occurrence.

[38] We conclude that sawtooth events are very often but not necessarily storm time phenomena and not all storms contain sawtooth events. The relationship is similar to substorms and storms. We also suggest sawtooth events, periodic substorms and single substorms can be considered as members of substorm family.

[39] **Acknowledgments.** This research is supported by the National Science Foundation through a GEM postdoctoral Support Award ATM-0725904 for Xia Cai and NASA grant NNX07AH23G. Partial support has also come from NSF grant AGS-1049403. We would thank LANL and GSFC OMNI Web sites for providing data online.

[40] Masaki Fujimoto thanks the reviewers for their assistance in evaluating this paper.

References

Akasofu, S.-I. (1964), The development of the auroral substorm, *Planet. Space Sci.*, *101*, 273.

Arnoldy, R. L., and K. W. Chan (1969), Particle substorms observed at the geostationary orbit, *J. Geophys. Res.*, *74*, 5019–5028, doi:10.1029/JA074i021p05019.

Baker, D. N., A. J. Klimas, R. L. McPherron, and J. Buechner (1990), The evolution from weak to strong geomagnetic activity: An interpretation in terms of deterministic chaos, *Geophys. Res. Lett.*, *17*, 41–44, doi:10.1029/GL017i001p00041.

Belian, R. D., T. E. Cayton, and G. D. Reeves (1995), Quasi-periodic global substorm-generated variations observed at geosynchronous orbit, in *Space Plasmas: Coupling Between Small and Medium Scale Processes*, *Geophys. Monogr. Ser.*, vol. 86, edited by M. Ashour-Abdalla and T. Chang and P. Dusenburg, p. 143, AGU, Washington, D. C.

Borovsky, J. E., B. Lavraud, and M. M. Kuznetsova (2009), Polar cap potential saturation, dayside reconnection, and changes to the magnetosphere, *J. Geophys. Res.*, *114*, A03224, doi:10.1029/2009JA014058.

Cai, X. (2007), Investigation of global periodic sawtooth oscillations observed in energetic particle flux at geosynchoronous orbit, Ph.D. thesis, 208 pp., Univ. of Mich., at Ann Arbor, 30 April.

Cai, X., and C. R. Clauer (2009), Investigation of the period of sawtooth events, *J. Geophys. Res.*, *114*, A06201, doi:10.1029/2008JA013764.

Cai, X., M. Henderson, and C. Clauer (2006a), A statistical study of magnetic dipolarization for sawtooth events and isolated substorms at geosynchronous orbit with goes data, *Ann. Geophys.*, *24*, 3481–3490.

Cai, X., C. Clauer, and A. Ridley (2006b), Statistical analysis of ionospheric potential patterns for isolated substorms and sawtooth events, *Ann. Geophys.*, *24*, 1,977–1,991.

Chapman, S., and J. Bartels (1940), *Geomagnetism*, Clarendon, Oxford, U. K.

Clauer, C. R., R. L. McPherron, C. Searls, and M. G. Kivelson (1981), Solar wind control of auroral zone geomagnetic activity, *Geophys. Res. Lett.*, *8*, 915, doi:10.1029/GL008i008p00915.

Clauer, C. R., X. Cai, D. Welling, A. DeJong, and M. G. Henderson (2006), Characterizing the 18 April 2002 storm-time sawtooth events using ground magnetic data, *J. Geophys. Res.*, *111*, A04S90, doi:10.1029/2005JA011099.

Daglis, I. A., and Y. Kamide (2003), The role of substorms in storm-time particle acceleration, in *Disturbances in Geospace: The Storm-Substorm Relationship*, *Geophys. Monogr. Ser.*, vol. 142, edited by A. S. Sharma, Y. Kamide, and G. S. Lakhina, p. 119, AGU, Washington, D. C.

DeJong, A. D., A. J. Ridley, and C. R. Clauer (2008), Balanced reconnection intervals: Four case studies, *Ann. Geophys.*, *26*, 3897–3912.

Dessler, A. J., and E. N. Parker (1959), Hydromagnetic theory of magnetic storms, *J. Geophys. Res.*, *64*, 2239–2252, doi:10.1029/JZ064i010p01643.

Fok, M.-C., T. E. Moore, and D. C. Delcourt (1999), Modeling of inner plasma sheet and ring current during substorms, *J. Geophys. Res.*, *104*, 14,557–14,569, doi:10.1029/1999JA900014.

Gonzalez, W. D., A. L. C. Gonzalez, and B. T. Tsurutani (1990), Dual-peak solar cycle distribution of intense geomagnetic storms, *Planet. Space Sci.*, *38*, 181–187, doi:10.1016/0032-0633(90)90082-2.

Gonzalez, W. D., J. A. Joselyn, Y. Kamide, H. W. Kroehl, G. Rostoker, B. T. Tsurutani, and V. M. Vasyliunas (1994), What is a geomagnetic storm?, *J. Geophys. Res.*, *99*, 5771–5792, doi:10.1029/93JA02867.

Gonzalez, W. D., B. T. Tsurutani, and A. L. C. Gonzalez (1999), Interplanetary origin of geomagnetic storms, *Space Sci. Rev.*, *88*, 529–562.

Henderson, M. G. (2004), The May 2-3, 1986 cdaw-9c interval: A sawtooth event, *Geophys. Res. Lett.*, *31*, L11804, doi:10.1029/2004GL019941.

Henderson, M. G., et al. (2006a), Substorms during the 10–11 August 2000 sawtooth event, *J. Geophys. Res.*, *111*, A06206, doi:10.1029/2005JA011366.

Henderson, M. G., G. D. Reeves, R. M. Skoug, M. F. Thomsen, M. H. Denton, S. B. Mende, T. J. Immel, P. C. Brandt, and H. J. Singer (2006b), Magnetospheric and auroral activity during the April 18, 2002 sawtooth event, *J. Geophys. Res.*, *111*, A01S90, doi:10.1029/2005JA011111.

Huang, C.-S., G. D. Reeves, J. E. Borovsky, R. M. Skoug, Z. Y. Pu, and G. Le (2003a), Periodic magnetospheric substorms and their relationship with solar wind variations, *J. Geophys. Res.*, *108*(A6), 1255, doi:10.1029/2002JA009704.

Huang, C.-S., J. C. Foster, G. D. Reeves, G. Le, H. U. Frey, C. J. Pollock, and J.-M. Jahn (2003b), Periodic magnetospheric substorms: Multiple space-based and ground-based instrumental observations, *J. Geophys. Res.*, *108*(A11), 1411, doi:10.1029/2003JA009992.

Huang, C.-S., J. C. Foster, L. P. Goncharenko, G. D. Reeves, J. L. Chau, K. Yumoto, and K. Kitamura (2004), Variations of low-latitude geomagnetic fields and *Dst* index caused by magnetospheric substorm, *J. Geophys. Res.*, *109*, A05219, doi:10.1029/2003JA010334.

Ilie, R., M. W. Liemohn, and A. Ridley (2010), The effect of smoothed solar wind inputs on global modeling results, *J. Geophys. Res.*, *115*, A01213, doi:10.1029/2009JA014443.

Kamide, Y., et al. (1998), Current understanding of magnetic storms: Storm-substorm relationships, *J. Geophys. Res.*, *103*, 17,705, doi:10.1029/98JA01426.

Kitamura, K., H. Kawano, S. Ohtani, A. Yoshikawa, and K. Yumoto (2005), Local time distribution of low and middle latitude ground magnetic disturbances at sawtooth injections of 18–19 April 2002, *J. Geophys. Res.*, *110*, A07208, doi:10.1029/2004JA010734.

Lee, D.-Y., L. Lyons, and K. Yumoto (2004), Sawtooth oscillations directly driven by solar wind dynamic pressure enhancements, *J. Geophys. Res.*, *109*, A04202, doi:10.1029/2003JA010246.

Liemohn, M. W., J. U. Kozyra, A. J. Ridley, M. F. Thomsen, M. G. Henderson, P. C. Brandt, and D. G. Mitchell (2007), Modeling the ring current response to a sawtooth oscillation event, *J. Atmos. Sol. Terr. Phys.*, *69*, 67, doi:10.1016/j.jastp.2006.07.016.

McPherron, R. L., and T.-S. Hsu (2002), A comparison of substorms occurring during magnetic storms with those occurring during quiet times, *J. Geophys. Res.*, *107*(A9), 1259, doi:10.1029/2001JA002008.

Nagai, T., M. Fujimoto, R. Nakamura, W. Baumjohann, A. Ieda, I. Shinohara, S. Machida, Y. Saito, and T. Mukai (2005), Solar wind control of the radial distance of the magnetic reconnection site in the magnetotail, *J. Geophys. Res.*, *110*, A09208, doi:10.1029/2005JA011207.

O'Brien, T., and R. McPherron (2000), An empirical phase-space analysis of ring current dynamics: Solar wind control of injection and decay, *J. Geophys. Res.*, *105*, 7707, doi:10.1029/1998JA000437.

Partamies, N., T. I. Pulkkinen, R. L. McPherron, K. McWilliams, C. R. Bryant, E. Tanskanen, H. J. Singer, G. D. Reeves, and M. F. Thomsen (2009), Statistical survey on sawtooth events, SMCs and isolated substorms, *Adv. Space Res.*, *44*, 376, doi:10.1016/j.asr.2009.03.013.

Pulkkinen, T. I., N. Partamies, R. L. McPherron, M. Henderson, G. D. Reeves, M. F. Thomsen, and H. J. Singer (2007), Comparative statistical analysis of storm time activations and sawtooth events, *J. Geophys. Res.*, *112*, A01205, doi:10.1029/2006JA012024.

Reeves, G. G., and M. G. Henderson (2001), The storm-substorm relationship: Ion injections in geosynchronous measurements and composite energetic neutral atom images, *J. Geophys. Res.*, *106*, 5833, doi:10.1029/2000JA003017.

Shaw, R. (1984), *The Dripping Faucet as a Model Chaotic System*, Aerial, Santa Cruz, Calif.

Tsurutani, B. T., and W. D. Gonzalez (2006), A new perspective of the relationship between substorms and magnetic storms, in *Advances in Geoscience*, vol. 8, *Solar Terrestrial*, p. 25, World Sci., Singapore.

Wanliss, J. A., and K. M. Showalter (2006), High-resolution global storm index: *Dst* versus *SYM-H*, *J. Geophys. Res.*, *111*, A02202, doi:10.1029/2005JA011034.

Weimer, D. R., and J. H. King (2008), Improved calculations of interplanetary magnetic field phase front angles and propagation time delays, *J. Geophys. Res.*, *113*, A01105, doi:10.1029/2007JA012452. (Correction to "improved calculations of imf phase-front angles and propagation time delays," *J. Geophys. Res.*, *113*, A07106, doi:10.1029/2008JA013075, 2008.)

Zhang, J., I. G. Richardson, and D. F. Webb (2008), Interplanetary origin of multiple-dip geomagnetic storms, *J. Geophys. Res.*, *113*, A00A12, doi:10.1029/2008JA013228.

X. Cai and C. R. Clauer, Bradley Department of Electrical and Computer Engineering, Virginia Tech, Blacksburg, VA 24061, USA. (xcai@vt.edu)

M. W. Liemohn, Department of Atmospheric, Oceanic and Space Sciences, University of Michigan, 2455 Hayward St., Ann Arbor, MI 48109-2143, USA.

J.-C. Zhang, Space Science Center, University of New Hampshire, 8 College Rd., Morse Hall, Durham, NH 03824, USA.